

Secure Beamforming for ISAC Systems Under Communication Eavesdropper and Sensing Eavesdropper

Tian Zhang, *Member, IEEE*, Zhirong Su, and Yueyi Dong
 tianzhang@sdnu.edu.cn

Abstract—Due to great efficiency improvement in resource and hardware space, integrated sensing and communication (ISAC) has gained much attention. In the paper, the physical layer security (PLS) of ISAC system under communication eavesdropper together with sensing eavesdropper is investigated. The system secrecy rate is maximized by transmit beamforming design of communication and sensing signals when taking sensing security, sensing performance and transmit power constraint into consideration. To deal with the formulated non-convex optimization problem, the successive convex approximation (SCA) together with the first-order Taylor expansion and semidefinite relaxation (SDR) is utilized. Additionally, it is theoretically validated that the SDR does not yield sub-optimality in the paper. Thereafter, an iterated joint secure beamforming algorithm against communication and sensing eavesdroppers is proposed. Simulation results validate the effectiveness and advance of the proposed scheme.

Index Terms—Integrated sensing and communication (ISAC), physical layer security (PLS), sensing security

I. INTRODUCTION

INTEGRATED sensing and communication (ISAC), which incorporates radar sensing and wireless communications in hardware sharing together with joint resource allocation manner, has been viewed as a promising technology for future 6G [1]. Sensing and communication can enhance each other, communication-aided sensing and sensing-aided communications are two main research aspects, which include physical layer, MAC layer, network and cross-layer design of ISAC, in academia and industry [2] [3]. In [4], coverage and rate analysis are carried out for ISAC networks, and a generalized stochastic geometry framework is introduced. In [5], network-layer delay provisioning for ISAC-unmanned aerial vehicle (UAV) networks under transient antenna misalignment is investigated. In [6], the channel modeling of ISAC towards 3GPP 6G standardization is studied. In [7], an analog assisted orthogonal-frequency-division-multiplexing (OFDM) receiver with ultra-low-rate analog-digital-converters (ADCs) is presented for ISAC. In [8], the trade-off between sensing and communication in ISAC is investigated, and a joint sensing and communication (JSC) beamforming framework is presented.

Due to the vulnerability of ISAC, security study plays a vital role. Specially, many efforts have been made on the physical-layer security (PLS) in ISAC systems. In [9], mitigating information leakage between communication and sensing in ISAC is considered, the partial characterization of the secrecy-distortion region is obtained. In [10], a power efficient secure ISAC optimization framework is formulated, and a beamforming design solution is proposed. In [11], the energy efficiency (EE) optimization is considered in secure full-duplex ISAC systems. In [12], a two-stage transmission protocol containing

beam sensing of channel state information (CSI) and secure communication is designed. In [13], predictive beamforming approach for secure ISAC with multiple aerial eavesdroppers is studied. In [14], a weighted optimization framework in near-field ISAC is designed by jointly maximizing the overall secrecy rate and reducing the Cramér-Rao bound (CRB) for target estimation. In [15], robust beamforming design is studied for secure near-field ISAC systems. In [16], secure and energy-efficient ISAC in low-altitude internet of things (IoT) is considered, and a game-theoretic deep reinforcement learning (DRL) framework with adaptive sensing is designed. In [17], joint dynamic tracking and robust secure beamforming is investigated in full-duplex ISAC systems. In [18], the achievable uplink rate maximization problem by joint optimizing the transmit beamforming and UAV trajectory is studied. In [19], secure precoding via interference exploitation in ISAC is considered. In [20], secure waveform design for multiple-input-multiple-output (MIMO) ISAC under the stochastic target impulse response (TIR) model is investigated. In [21], a joint secure sensing and communication framework in ISAC-assisted covert transmission is proposed.

In above works, the security scenarios constructed for ISAC systems primarily focus on threats posed by communication eavesdroppers. However, both communication services and sensing services are available in ISAC systems, allowing users within ISAC to choose and subscribe to different services based on their needs. Consequently, users subscribed to sensing services can utilize ISAC echo signals to extract sensing information related to targets or the surrounding environment. When confidential targets (e.g., those performing covert reconnaissance missions) exist within the system and do not wish their movements to be detected by nearby devices, users capable of extracting sensing information may pose potential sensing security threats. Thus, for ISAC systems, ensuring the security of sensing information is as important as guaranteeing communication information security. However, scenarios involving sensing security threats in ISAC systems have not yet been thoroughly investigated. In [22], secure cell-free ISAC in the existence of information and sensing eavesdroppers is considered. In [23], beamforming design to enhance the sensing security in ISAC systems is studied. In [24], a sensing-secure ISAC signaling is proposed by ambiguity function engineering for impairing unauthorized sensing.

In the paper, we investigate an ISAC system in the presence of both communication and sensing eavesdroppers. The legitimate communication users (CUs) act as potential sensing eavesdroppers, and the sensing target plays the role of communication eavesdropper simultaneously. The beamforming for

maximizing communication secrecy rate under the sensing performance and sensing security guarantees is studied.

The main contributions of the paper can be summarized as follows.

- In an ISAC system under communication eavesdropper as well as sensing eavesdropper, the beamforming design with maximal down-link communication secrecy rate is investigated. The sensing security, the sensing performance, and the transmit power are taken into consideration. Accordingly, a non-convex optimization problem is formulated, where the sum of down-link communication secrecy rate, referred to as the system secrecy rate, is viewed as the objective function, the communication signal & sensing signal beamforming covariance matrices are the optimizing variables, and the sensing security, the sensing performance, the transmit power introduce optimization constraints.
- To tackle the formulated non-convex problem, the successive convex approximation (SCA) is applied. First, the non-convex objective function is transformed to an approximated convex version by employing the inverse relationship between logarithmic and exponential functions as well as the first-order Taylor expansion. Then employing semidefinite relaxation (SDR), we arrive at the approximated convex optimization problem, which is iteratively addressed in the SCA. By the way, it is mathematically verified that the SDR does not produce sub-optimality for the corresponding problem in the paper.
- Iterated secure beamforming algorithm against communication eavesdropper and sensing eavesdropper is presented accordingly. Numerical results demonstrate the effectiveness and advance of the proposed scheme.

The rest of the paper is structured as follows. Section II describes the considered system, communication model, sensing model, security model, and the optimization problem are given. Next, the solution of the formulated non-convex optimization problem is derived and an iterative algorithm is proposed in Section III. Numerical results are given in Section IV. Finally, Section V concludes the whole paper.

Notations: $[\cdot]^T$ and $(\cdot)^H$ are the transpose and conjugate transpose, respectively. $\text{Tr}(\cdot)$ and $\text{rank}(\cdot)$ denote the trace and rank, respectively. $\mathbb{E}[\cdot]$ is the expectation. $\mathcal{CN}(\mu, \sigma^2)$ represents the normal distribution with mean μ and variance σ^2 . $[z]^+ = \max\{z, 0\}$.

II. SYSTEM MODEL AND PROBLEM FORMULATION

Consider an ISAC scenario as in Fig. 1. The DFRC base station (BS) with N_t antennas transmits confidential information to K single-antenna CUs while simultaneously sensing a confidential target. The communication information is private to the sensing target, and the sensing information is private to the CU as well. For confidentiality, the scope of awareness for both types of information should be kept as small as possible. However, since the CUs can receive the ISAC echo signals reflected by the sensing target, they act as potential eavesdroppers of sensing. Meanwhile, the ISAC signal transmitted toward the sensing target also contains

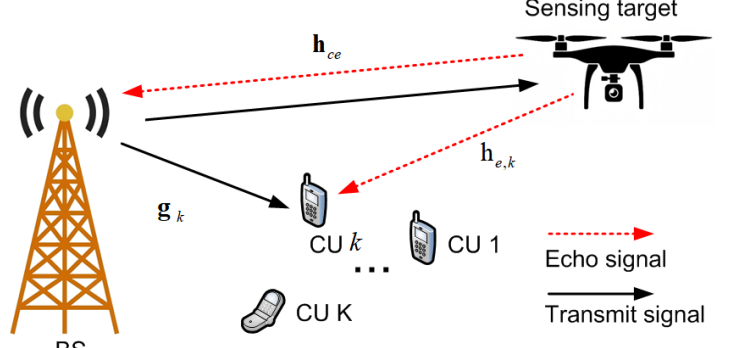


Fig. 1. System model

the communication information, so the sensing target acts as a potential communication eavesdropper. In the paper, the security of both communication and sensing information is ensured through the design of beamforming for the transmitted signals at the BS. In addition, it is assumed that the BS can access the CSI from all nodes.

A. Communications Model

The signal transmitted by the DFRC BS, \mathbf{x} , includes a communication signal for serving multiple CUs and a sensing signal for detecting the sensing target, specifically it can be expressed by

$$\mathbf{x} = \mathbf{W}\mathbf{c} + \mathbf{s} = \sum_{k=1}^K \mathbf{w}_k c_k + \mathbf{s}, \quad (1)$$

where $\mathbf{c} = [c_1, \dots, c_K]^T \in \mathbb{C}^{K \times 1}$ represents the communication symbols transmitted from the BS to the CUs, satisfying $\mathbb{E}[\mathbf{c}\mathbf{c}^H] = \mathbf{I}_K$, $\mathbf{W} = [\mathbf{w}_1, \dots, \mathbf{w}_K] \in \mathbb{C}^{N_t \times K}$ denotes the communication beamforming matrix, and $k \in \{1, 2, \dots, K\}$. $\mathbf{s} \in \mathbb{C}^{N_t \times 1}$ is the sensing signal, which can also serve as artificial noise to interfere with potential eavesdroppers in the system, satisfying $\mathbf{s} \sim \mathcal{CN}(\mathbf{0}, \mathbf{S})$. It is assumed that the communication signal and the sensing signal in \mathbf{x} are mutually independent. The covariance matrix of the transmitted signal from the BS, \mathbf{R} , can be given by

$$\mathbf{R} = \mathbb{E}[\mathbf{x}\mathbf{x}^H] = \sum_{k=1}^K \mathbf{w}_k \mathbf{w}_k^H + \mathbf{S}, \quad (2)$$

where $\mathbf{S} = \mathbb{E}[\mathbf{s}\mathbf{s}^H]$ with $\mathbf{S} = \mathbf{S}^H$ & $\mathbf{S} \succeq \mathbf{0}$. Let $\mathbf{Q}_k = \mathbf{w}_k \mathbf{w}_k^H$, then the matrix \mathbf{Q}_k should simultaneously satisfy $\mathbf{Q}_k \succeq \mathbf{0}$, $\mathbf{Q}_k = \mathbf{Q}_k^H$, and $\text{rank}(\mathbf{Q}_k) = 1$. Thereafter, we have

$$\mathbf{R} = \sum_{k=1}^K \mathbf{Q}_k + \mathbf{S}. \quad (3)$$

The total transmit power at the BS can be written as

$$P_{\text{BS}} = \text{Tr}(\mathbf{R}) = \text{Tr} \left(\sum_{k=1}^K \mathbf{Q}_k + \mathbf{S} \right). \quad (4)$$

The signal received by the k -th CU, y_k , includes the direct ISAC signal from the BS and the ISAC echo signal reflected by the sensing target, can be given by

$$y_k = \mathbf{g}_k^H \mathbf{x} + h_{\text{se},k} \mathbf{x} + n_k \quad (5)$$

$$= (\mathbf{g}_k^H + h_{\text{se},k}) \mathbf{w}_k c_k + (\mathbf{g}_k^H + h_{\text{se},k}) \sum_{i=1, i \neq k}^K \mathbf{w}_i c_i \\ + \left(\mathbf{g}_k^H + h_{\text{se},k} \right) \mathbf{s} + n_k, \quad (6)$$

where $n_k \sim \mathcal{CN}(0, \sigma_k^2)$ is the additive white Gaussian noise (AWGN) at the CU k receiver, $\mathbf{g}_k \in \mathbb{C}^{N_t \times 1}$ is the channel vector of the direct link between the BS and the k -th CU, $h_{\text{se},k} \in \mathbb{C}^{1 \times N_t}$ is the channel vector of the cascaded link from the BS to the sensing target to the k -th CU, i.e.,

$$h_{\text{se},k} = h_{\text{e},k} \mathbf{h}_{\text{ce}}^H,$$

where $h_{\text{e},k}$ denotes the channel between the sensing target and the k -th CU, $\mathbf{h}_{\text{ce}} \in \mathbb{C}^{N_t \times 1}$ is the channel vector from the BS to the sensing target.

Both the direct link signal and the echo signal contain the useful communication information c_k for CU k . After defining

$$\mathbf{h}_k = \mathbf{g}_k^H + h_{\text{se},k}$$

with $\mathbf{h}_k \in \mathbb{C}^{1 \times N_t}$, the communication SINR at the k -th CU can be derived as

$$\text{SINR}_{u,k} = \frac{|\mathbf{h}_k \mathbf{w}_k|^2}{\sigma_k^2 + \sum_{i=1, i \neq k}^K |\mathbf{h}_k \mathbf{w}_i|^2 + \mathbb{E}[|\mathbf{h}_k \mathbf{s}|^2]} \quad (7)$$

$$= \frac{\mathbf{h}_k \mathbf{Q}_k \mathbf{h}_k^H}{\sigma_k^2 + \sum_{i=1, i \neq k}^K \mathbf{h}_k \mathbf{Q}_i \mathbf{h}_k^H + \mathbf{h}_k \mathbf{S} \mathbf{h}_k^H}. \quad (8)$$

Furthermore, the achievable rate of the k -th CU can be expressed as

$$R_{u,k} = \log_2(1 + \text{SINR}_{u,k}). \quad (9)$$

B. Sensing Model

The echo signal received at the BS, denoted as \mathbf{y}_b , can be written as

$$\mathbf{y}_b = \mathbf{H}_{\text{ce}} \mathbf{x} + \mathbf{n}_b = \mathbf{H}_{\text{ce}} \mathbf{s} + \sum_{k=1}^K \mathbf{H}_{\text{ce}} \mathbf{w}_k c_k + \mathbf{n}_b, \quad (10)$$

where

$$\mathbf{H}_{\text{ce}} = \mathbf{h}_{\text{ce}} \mathbf{h}_{\text{ce}}^H,$$

$\mathbf{H}_{\text{ce}} \in \mathbb{C}^{N_t \times N_t}$ represents the cascaded channel from the BS to the sensing target and back to the BS, $\mathbf{n}_b \sim \mathcal{CN}(\mathbf{0}, \sigma_b^2 \mathbf{I}_{N_t})$ is the AWGN for the ISAC signal detecting the sensing target.

Thereafter, viewing the transmitted communication information \mathbf{c} as an interference signal, the sensing signal-clutter-noise ratio (SCNR) of the ISAC echo signal at the BS, SCNR_b , can be given by

$$\text{SCNR}_b = \frac{\mathbb{E}[\|\mathbf{H}_{\text{ce}} \mathbf{s}\|^2]}{\sigma_b^2 + \sum_{k=1}^K \|\mathbf{H}_{\text{ce}} \mathbf{w}_k\|^2} \quad (11)$$

$$= \frac{\text{Tr}(\mathbf{H}_{\text{ce}} \mathbf{S} \mathbf{H}_{\text{ce}}^H)}{\sigma_b^2 + \sum_{k=1}^K \text{Tr}(\mathbf{H}_{\text{ce}} \mathbf{Q}_k \mathbf{H}_{\text{ce}}^H)}. \quad (12)$$

The sensing performance of the ISAC system is measured by SCNR_b .

C. Security Model

Communication Security: The eavesdropped signal received by the communication eavesdropper (i.e., the sensing target), y_t , can be given by

$$y_t = \mathbf{h}_{\text{ce}}^H \mathbf{x} + n_t = \sum_{k=1}^K \mathbf{h}_{\text{ce}}^H \mathbf{w}_k c_k + \mathbf{h}_{\text{ce}}^H \mathbf{s} + n_t, \quad (13)$$

where $n_t \sim \mathcal{CN}(0, \sigma_t^2)$ is the AWGN at the communication eavesdropper. When the potential communication eavesdropper attempts to intercept the communication information of the k -th CU, besides the interference from other users' communication information, the sensing signal \mathbf{s} also acts as artificial noise to interfere with its eavesdropping. The SINR for the potential communication eavesdropper intercepting communication information of the k -th CU, $\text{SINR}_{t,k}$, can be expressed as

$$\text{SINR}_{t,k} = \frac{|\mathbf{h}_{\text{ce}}^H \mathbf{w}_k|^2}{\sigma_t^2 + \mathbb{E}[|\mathbf{h}_{\text{ce}}^H \mathbf{s}|^2] + \sum_{i=1, i \neq k}^K |\mathbf{h}_{\text{ce}}^H \mathbf{w}_i|^2}. \quad (14)$$

Furthermore, the achievable rate for the potential communication eavesdropper intercepting the information of the k -th CU can be derived by

$$R_{t,k} = \log_2(1 + \text{SINR}_{t,k}). \quad (15)$$

Accordingly, the system secrecy rate of the ISAC is given as

$$\text{SR} = \sum_{k=1}^K [R_{u,k} - R_{t,k}]^+. \quad (16)$$

Remark: The system secrecy rate is defined as the sum secrecy rate of the downlink in the ISAC system.

Sensing Security: A potential sensing eavesdropper (i.e., a CU) has the capability to exploit the ISAC echo signal reflected by the sensing target to extract sensing information. Therefore, similar to the BS, the quality of sensing information eavesdropping by a potential sensing eavesdropper can also be measured by the sensing SCNR. The potential sensing eavesdropper treats the communication information of other users as interference in the echo signal. The SCNR of the echo signal at the k -th sensing eavesdropper can be expressed as

$$\text{SCNR}_{u,k} = \frac{\mathbb{E}[|h_{\text{se},k} \mathbf{s}|^2] + |h_{\text{se},k} \mathbf{w}_k|^2}{\sigma_k^2 + \sum_{i=1, i \neq k}^K |h_{\text{se},k} \mathbf{w}_i|^2} \\ = \frac{h_{\text{se},k} \mathbf{S} h_{\text{se},k}^H + h_{\text{se},k} \mathbf{Q}_k h_{\text{se},k}^H}{\sigma_k^2 + \sum_{i=1, i \neq k}^K h_{\text{se},k} \mathbf{Q}_k h_{\text{se},k}^H}. \quad (17)$$

D. Problem Formulation

It is aimed to maximize the sum secrecy rate of the downlink in the ISAC system, by viewing the communication signal beamforming covariance matrices $\{\mathbf{Q}_k\}_{k=1}^K$ and the sensing signal beamforming covariance matrix \mathbf{S} as the optimizing

variables. Additionally, to ensure the sensing performance and sensing security, the SCNRs of the echo signal at the BS and at the sensing eavesdropper are taken as constraints. In addition, the total transmit power of the BS is also constrained. The beamforming design for maximizing the system secrecy rate with guaranteed sensing performance and sensing security in the ISAC downlink can be formulated as

$$(P1) \quad \max_{\{\mathbf{Q}_k\}_{k=1}^K, \mathbf{S}} \text{SR} \quad (18)$$

s.t.

$$\text{SCNR}_{u,k} \leq \gamma_{\text{se}}, \quad \forall k \quad (19)$$

$$\text{SCNR}_b \geq \gamma_s \quad (20)$$

$$P_{\text{BS}} \leq P \quad (21)$$

$$\text{rank}(\mathbf{Q}_k) = 1, \quad \forall k \quad (22)$$

$$\mathbf{Q}_k \succeq 0, \quad \mathbf{Q}_k = \mathbf{Q}_k^H, \quad \forall k \quad (23)$$

$$\mathbf{S} \succeq 0, \quad \mathbf{S} = \mathbf{S}^H. \quad (24)$$

Equation (19) is the sensing security constraint with γ_{se} being the upper limit of the SCNR at the system's sensing eavesdropper, Eq. (20) is the sensing performance constraint with γ_s representing the lower limit of the SCNR at the BS, and P denotes the maximum transmit power at the BS. According to Eq. (16), the term inside the summation in the objective function involves the subtraction of two $\log_2(\cdot)$ functions, each containing a fractional form with respect to the optimization variables, making the objective function non-convex. Additionally, Eq. (22) is a non-convex constraint. In summary, (P1) is a non-convex optimization problem, and it is challenging to obtain the solution directly.

III. PROBLEM SOLUTION AND ALGORITHM DESIGN

In this section, we grapple with the formulated non-convex problem in two steps. First, the objective function is manipulated in the SCA framework together with the first-order Taylor expansion. Then the SDR, which provokes no sub-optimality of corresponding problem, is deployed for convexity. Accordingly we reach an approximated convex optimization problem for SCA iteration. Finally, based on the mathematical analysis, an iterative beamforming algorithm against communication & sensing eavesdroppers is derived.

Let $m_1 = \frac{1}{\sigma_k^2}$, $m_2 = \frac{1}{\sigma_t^2}$, and $m_3 = \frac{1}{\sigma_b^2}$, (P1) can be re-

written as

$$(P2) \quad \max_{\{\mathbf{Q}_k\}_{k=1}^K, \mathbf{S}} \sum_{k=1}^K f(\mathbf{Q}_k, \mathbf{S}) \quad (25)$$

$$\text{s.t.} \quad (26)$$

$$m_1 (\mathbf{h}_{\text{se},k} \mathbf{S} \mathbf{h}_{\text{se},k}^H + \mathbf{h}_{\text{se},k} \mathbf{Q}_k \mathbf{h}_{\text{se},k}^H) \leq \gamma_{\text{se}} \left[1 + m_1 \sum_{i=1, i \neq k}^K \mathbf{h}_{\text{se},i} \mathbf{Q}_k \mathbf{h}_{\text{se},i}^H \right], \quad \forall k, \quad (27)$$

$$m_3 \text{Tr}(\mathbf{H}_{\text{ce}} \mathbf{S} \mathbf{H}_{\text{ce}}^H) \geq \gamma_s \left[1 + m_3 \sum_{k=1}^K \text{Tr}(\mathbf{H}_{\text{ce}} \mathbf{Q}_k \mathbf{H}_{\text{ce}}^H) \right], \quad (28)$$

$$\text{Tr} \left(\sum_{k=1}^K \mathbf{Q}_k + \mathbf{S} \right) \leq P, \quad (29)$$

$$\text{Eq. (22), Eq. (23), Eq. (24)}$$

where

$$f(\mathbf{Q}_k, \mathbf{S})$$

$$= \log_2 \frac{1 + m_1 (\mathbf{h}_k \mathbf{Q}_k \mathbf{h}_k^H + \sum_{i=1, i \neq k}^K \mathbf{h}_k \mathbf{Q}_i \mathbf{h}_k^H + \mathbf{h}_k \mathbf{S} \mathbf{h}_k^H)}{1 + m_1 (\sum_{i=1, i \neq k}^K \mathbf{h}_k \mathbf{Q}_i \mathbf{h}_k^H + \mathbf{h}_k \mathbf{S} \mathbf{h}_k^H)} - \log_2 \frac{1 + m_2 (\mathbf{h}_{\text{ce}}^H \mathbf{Q}_k \mathbf{h}_{\text{ce}} + \sum_{i=1, i \neq k}^K \mathbf{h}_{\text{ce}}^H \mathbf{Q}_i \mathbf{h}_{\text{ce}} + \mathbf{h}_{\text{ce}}^H \mathbf{S} \mathbf{h}_{\text{ce}})}{1 + m_2 (\sum_{i=1, i \neq k}^K \mathbf{h}_{\text{ce}}^H \mathbf{Q}_i \mathbf{h}_{\text{ce}} + \mathbf{h}_{\text{ce}}^H \mathbf{S} \mathbf{h}_{\text{ce}})}. \quad (30)$$

In the paper, we transform the non-convex objective function to an approximated convex version by leveraging the inverse relationship between logarithmic and exponential functions. Specifically, we introduce $\{\tau_k\}_{k=1}^K$, $\{\varepsilon_k\}_{k=1}^K$, u , and $\{v_k\}_{k=1}^K$ as auxiliary variables, and then use the exponential functions corresponding to these auxiliary variables to sequentially replace the numerator and denominator of the first fractional term and the second fractional term in the objective function, i.e.,

$$e^{\tau_k} \rightarrow 1 + m_1 \left(\mathbf{h}_k \mathbf{S} \mathbf{h}_k^H + \sum_{i=1}^K \mathbf{h}_k \mathbf{Q}_i \mathbf{h}_k^H \right), \quad \forall k, \quad (31)$$

$$e^{\varepsilon_k} \rightarrow 1 + m_1 \left(\mathbf{h}_k \mathbf{S} \mathbf{h}_k^H + \sum_{i=1, i \neq k}^K \mathbf{h}_k \mathbf{Q}_i \mathbf{h}_k^H \right), \quad \forall k, \quad (32)$$

$$e^u \rightarrow 1 + m_2 \left(\mathbf{h}_{\text{ce}}^H \mathbf{S} \mathbf{h}_{\text{ce}} + \sum_{i=1}^K \mathbf{h}_{\text{ce}}^H \mathbf{Q}_i \mathbf{h}_{\text{ce}} \right), \quad (33)$$

and

$$e^{v_k} \rightarrow 1 + m_2 \left(\mathbf{h}_{\text{ce}}^H \mathbf{S} \mathbf{h}_{\text{ce}} + \sum_{i=1, i \neq k}^K \mathbf{h}_{\text{ce}}^H \mathbf{Q}_i \mathbf{h}_{\text{ce}} \right), \quad \forall k. \quad (34)$$

Thereafter, $f(\mathbf{Q}_k, \mathbf{S})$ is transformed into

$$\log_2 e^{\tau_k} - \log_2 e^{\varepsilon_k} - \log_2 e^u + \log_2 e^{v_k}.$$

Using the change of base formula for logarithms, the first term $\log_2 e^{\tau_k}$ becomes $\tau_k / \ln 2$. Since $\ln 2$ is a constant and does

not affect the solution of the optimization problem (P2), it can be ignored, i.e., $\log_2 e^{\tau_k}$ is written as τ_k . The same actions are applied to the other auxiliary variables e^{ε_k} , e^u , and e^{v_k} . After the above replacement, the objective function is expressed as

$$\max_{\{\mathbf{Q}_k\}_{k=1}^K, \mathbf{S}, u, \{\tau_k, \varepsilon_k, v_k\}_{k=1}^K} \sum_{k=1}^K (\tau_k - \varepsilon_k - u + v_k). \quad (35)$$

The objective function is convex with respect to the auxiliary variables. Meanwhile, the introduced auxiliary variables are subject to

$$e^{\tau_k} \leq 1 + m_1 \left(\mathbf{h}_k \mathbf{S} \mathbf{h}_k^H + \sum_{i=1}^K \mathbf{h}_k \mathbf{Q}_i \mathbf{h}_k^H \right), \quad \forall k, \quad (36)$$

$$e^{\varepsilon_k} \geq 1 + m_1 \left(\mathbf{h}_k \mathbf{S} \mathbf{h}_k^H + \sum_{i=1, i \neq k}^K \mathbf{h}_k \mathbf{Q}_i \mathbf{h}_k^H \right), \quad \forall k, \quad (37)$$

$$e^u \geq 1 + m_2 \left(\mathbf{h}_{\text{ce}}^H \mathbf{S} \mathbf{h}_{\text{ce}} + \sum_{i=1}^K \mathbf{h}_{\text{ce}}^H \mathbf{Q}_i \mathbf{h}_{\text{ce}} \right), \quad (38)$$

and

$$e^{v_k} \leq 1 + m_2 \left(\mathbf{h}_{\text{ce}}^H \mathbf{S} \mathbf{h}_{\text{ce}} + \sum_{i=1, i \neq k}^K \mathbf{h}_{\text{ce}}^H \mathbf{Q}_i \mathbf{h}_{\text{ce}} \right), \quad \forall k. \quad (39)$$

Among the above four constraints, the sets represented by constraints (36) and (39) are convex, while the sets represented by constraints (37) and (38) are non-convex. To address the non-convexity of these inequalities, we process the exponential functions on the left-hand side by using SCA. The first-order Taylor expansion of the function is utilized as the surrogate function in the SCA. The first-order Taylor expansions of e^{ε_k} and e^u at $\varepsilon_k^{(n)}$ and $u_k^{(n)}$, respectively, are expressed as

$$e^{\varepsilon_k} \geq e^{\varepsilon_k^{(n)}} \left(1 + \varepsilon_k - \varepsilon_k^{(n)} \right), \quad (40)$$

and

$$e^u \geq e^{u^{(n)}} \left(1 + u - u^{(n)} \right). \quad (41)$$

Then, the non-convex constraints (37) and (38) can be transformed into

$$e^{\varepsilon_k^{(n)}} \left(1 + \varepsilon_k - \varepsilon_k^{(n)} \right) \geq 1 + m_1 \left(\mathbf{h}_k \mathbf{S} \mathbf{h}_k^H + \sum_{i=1, i \neq k}^K \mathbf{h}_k \mathbf{Q}_i \mathbf{h}_k^H \right) \quad (42)$$

and

$$e^{u^{(n)}} \left(1 + u - u^{(n)} \right) \geq 1 + m_2 \left(\mathbf{h}_{\text{ce}}^H \mathbf{S} \mathbf{h}_{\text{ce}} + \sum_{i=1}^K \mathbf{h}_{\text{ce}}^H \mathbf{Q}_i \mathbf{h}_{\text{ce}} \right), \quad (43)$$

where $\varepsilon_k^{(n)}$ and $u^{(n)}$ are the solutions at the n -th iteration. Consequently, the optimization problem (P2) can be transformed into problem (P3).

$$\begin{aligned} \text{(P3)} \quad & \max_{\{\mathbf{Q}_k\}_{k=1}^K, \mathbf{S}, u, \{\tau_k, \varepsilon_k, v_k\}_{k=1}^K} \sum_{k=1}^K (\tau_k - \varepsilon_k - u + v_k) \quad (44) \\ & \text{s.t.} \\ & \text{Eq. (22), Eq. (23), Eq. (24)} \\ & \text{Eq. (27), Eq. (28), Eq. (29)} \\ & \text{Eq. (36), Eq. (39), Eq. (42), Eq. (43)} \end{aligned}$$

Remark: Compared to these schemes, in which the fractional programming (FP) method is applied to handle each logarithmic function separately, with each requiring two rounds of FP processing, we achieve linearization of the objective function in a single step.

Due to the rank-one constraint (22), the problem (P3) remains non-convex. Then we have Lemma 1.

Lemma 1: Given $P > 0$, the solution of (P3) can be obtained by solving the following convex optimization problem (P4).

$$\begin{aligned} \text{(P4)} \quad & \max_{\{\mathbf{Q}_k\}_{k=1}^K, \mathbf{S}, u, \{\tau_k, \varepsilon_k, v_k\}_{k=1}^K} \sum_{k=1}^K (\tau_k - \varepsilon_k - u + v_k) \quad (45) \\ & \text{s.t.} \\ & \text{Eq. (23), Eq. (24)} \\ & \text{Eq. (27), Eq. (28), Eq. (29)} \\ & \text{Eq. (36), Eq. (39), Eq. (42), Eq. (43)} \end{aligned}$$

Proof: See Appendix. ■

Remark: We employ the SDR method by temporarily ignoring the rank-one constraints. The resulting semidefinite programming (SDP) problem (P4) is convex and can be solved efficiently. Then, according to Lemma 1, it is shown that the optimal \mathbf{Q}_k obtained from the relaxed SDP problem still satisfies the rank-one constraint. The SDR does NOT incur sub-optimality. There is no need to adopt methods such as Gaussian randomization or eigenvalue decomposition to reconstruct a rank-one solution, thereby reducing the computational complexity.

Thereafter, we design the secure beamforming algorithm, as Algorithm 1, to give the maximal system secrecy rate of communications with guaranteed sensing security and sensing performance. Regarding the convergence of the algorithm, it is determined by the relative change Δ_f in the objective function value, which is obtained in the current iteration compared to the previous iteration. The algorithm converges when Δ_f is less than or equal to the convergence tolerance. Additionally, in the SCA, the initial points $\varepsilon_k^{(0)}$ and $u^{(0)}$ is crucial. Initial values that are too large or too small may lead to issues such as slow algorithm convergence, numerical instability, or even infeasibility.

Algorithm 1: Secure Beamforming Algorithm Against Communication Eavesdropper and Sensing Eavesdropper

- 1) **Initialize:** Initial points $\varepsilon_k^{(0)}$ and $u^{(0)}$, initial objective function value $f^{(0)}$, convergence tolerance δ , iteration count $n = 0$.
- 2) **While** $\Delta_f > \delta$
- 3) Substitute $\varepsilon_k^{(n)}$ and $u^{(n)}$ into Eqs (42) and (43), solve the convex optimization problem (P4) to derive the solution $\tau_k, \varepsilon_k, u, v_k, \mathbf{S}$, and $\{\mathbf{Q}_k\}_{k=1}^K$.
- 4) Compute
$$f^{(n+1)} = \sum_{k=1}^K (\tau_k - \varepsilon_k - u + v_k).$$
- 5) Update $\Delta_f = \left| \frac{f^{(n+1)} - f^{(n)}}{f^{(n)}} \right|$.
- 6) Update $n = n + 1$.
- 7) Update $\varepsilon_k^{(n)} = \varepsilon_k$.
- 8) Update $u^{(n)} = u$.
- 9) **End While**
- 10) **Output:** The solution $\mathbf{S}^* = \mathbf{S}$, and $\{\mathbf{Q}_k^*\}_{k=1}^K = \{\mathbf{Q}_k\}_{k=1}^K$.

IV. NUMERICAL RESULTS

The channel between the sensing target and the k -th CU is given by

$$h_{e,k} = \beta_{e,k} e^{j\phi_k}, \quad (46)$$

where $\beta_{e,k}$ is the path loss between the sensing target and the k -th CU. The channel link between the BS and the sensing target is given by

$$\mathbf{h}_{ce} = \beta_{ce} \mathbf{a}(\theta_t), \quad (47)$$

where β_{ce} is related to the radar cross section (RCS) of the sensing target together with the path loss between the BS and the sensing target, $\mathbf{a}(\theta_t)$ is the array steering vector, which can be expressed as (in far-field circumstance)

$$\mathbf{a}(\theta_t) = \left[1, e^{j2\pi \frac{d}{\lambda} \sin(\theta_t)}, \dots, e^{j2\pi (N_t-1) \frac{d}{\lambda} \sin(\theta_t)} \right]^T, \quad (48)$$

where θ_t denotes the angle of arrival (AoA) of the sensing target, d represents the distance between two adjacent antennas at the BS, and λ denotes the wavelength. Typically $d/\lambda = 0.5$. The communication channel links between the BS and CUs are modeled as Rayleigh channels. For large-scale fading, the distance-dependent path loss model $PL(d_s)$ can be expressed as

$$PL(d_s) = C_0 \left(\frac{d_0}{d_s} \right)^l, \quad (49)$$

where $d_0 = 1\text{m}$ is the reference distance, the reference path loss is $C_0 = -30\text{dB}$, d_s denotes the link distance, and l is the path loss exponent. The path loss exponent between the BS and CUs is $l = 3.3$, between the BS and the sensing target is $l = 2$, and between the sensing target and CUs is $l = 2.3$. Unless otherwise specified, the default simulation parameters are set as shown in Table I.

Fig. 2 depicts the convergence performance of the proposed beamforming algorithm. The maximum transmit power of

TABLE I
SIMULATION PARAMETERS

Parameter	Value
Number of CUs K	3
Sensing target AoA θ_t	0°
RCS	1 m^2
Noise power of CUs σ_k^2	-80 dBm
Noise power of sensing target σ_t^2	-80 dBm
Noise power of BS σ_b^2	-100 dBm
Distance between CU 1 and BS $d_{BU,1}$	30 m
Distance between CU 2 and BS $d_{BU,2}$	30 m
Distance between CU 3 and BS $d_{BU,3}$	30 m
Distance between CU 1 and the sensing target $d_{UT,1}$	25 m
Distance between CU 2 and the sensing target $d_{UT,2}$	25 m
Distance between CU 3 and the sensing target $d_{UT,3}$	30 m
Distance between BS and the sensing target d_{BT}	50 m
Convergence tolerance δ	0.001

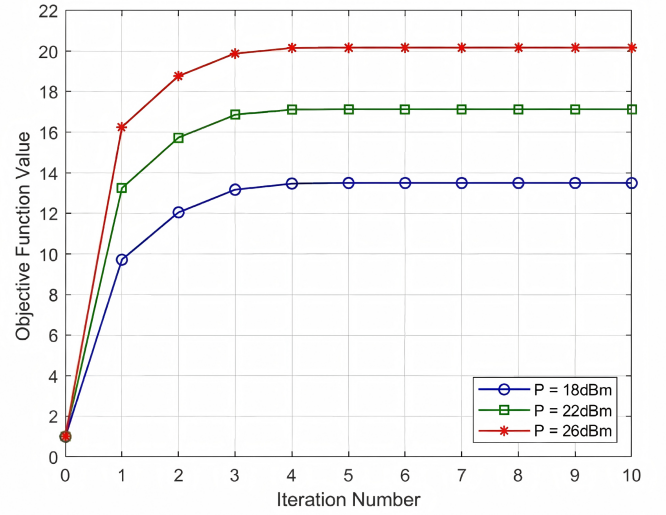


Fig. 2. Convergence performance

the BS is set as $P = 18\text{dBm}$, $P = 22\text{dBm}$, and $P = 26\text{dBm}$. It can be observed that under different maximum BS transmit power conditions, the objective function value essentially stabilizes after the fourth iterations, demonstrating the good convergence performance of the designed algorithm. To investigate the relationship between sensing security and sensing performance, the relationship between the BS SCNR threshold and the sensing SCNR at the sensing eavesdropper, as well as the relationship between the BS SCNR threshold and the feasibility probability, are simulated in Fig. 3 and Fig. 4, respectively. In each simulation, different sensing security thresholds γ_{se} are set. The BS antenna number $N_t = 8$, maximum transmit power of the BS $P = 18\text{ dBm}$. The SCNR at the 3 sensing eavesdroppers are denoted as “SCNR1”, “SCNR2”, and “SCNR3”. The feasibility probability refers to the probability that the proposed scheme can simultaneously meet all pre-defined quality-of-service requirements. From Fig. 3, it can be observed that although the SCNR at the sensing eavesdroppers gradually increases with larger BS SCNR threshold, the SCNR in the proposed scheme remains below γ_{se} (i.e., threshold on sensing security). In contrast, the scheme without sensing security constraint continues to

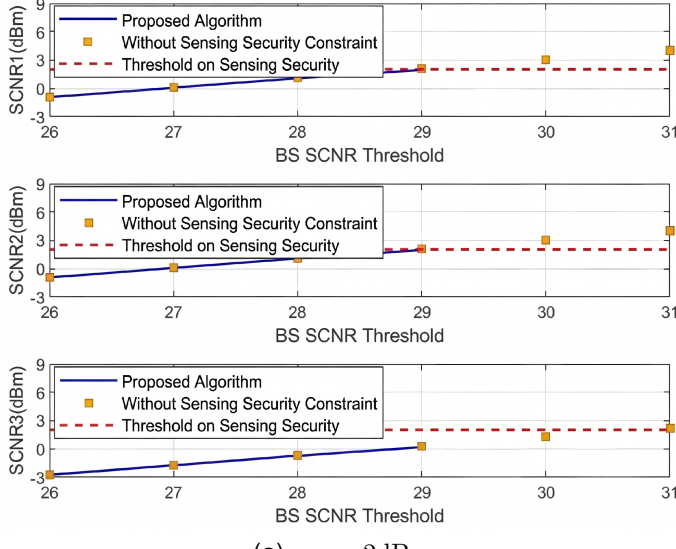
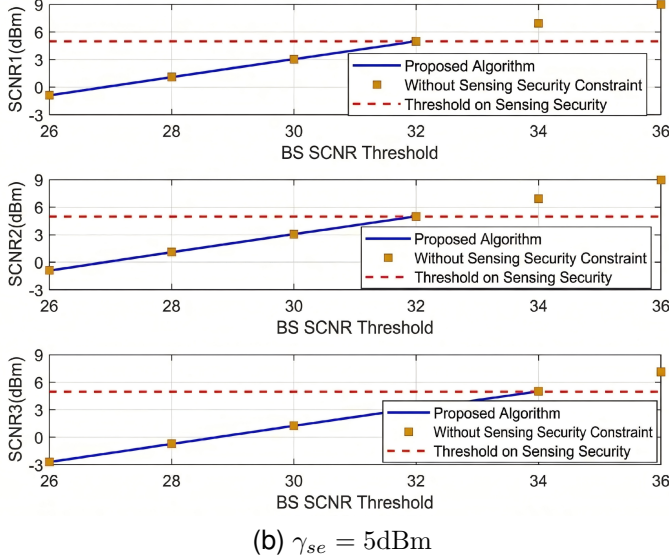
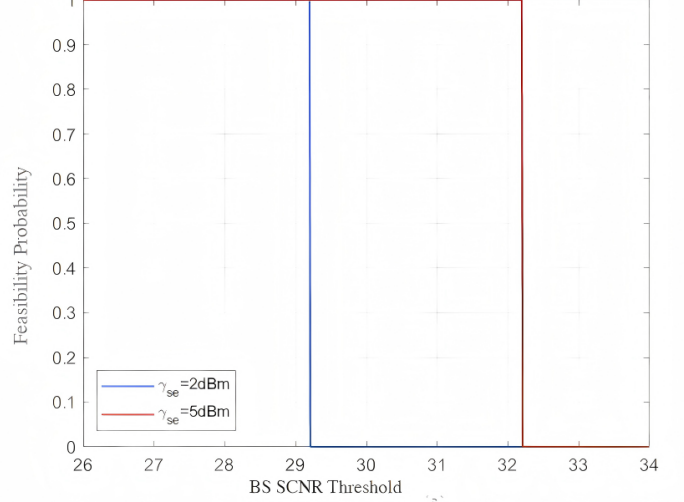
(a) $\gamma_{se} = 2\text{dBm}$ (b) $\gamma_{se} = 5\text{dBm}$

Fig. 3. Sensing SCNR at the sensing eavesdropper v.s. BS SCNR threshold

increase above γ_{se} . This demonstrates the effectiveness of the sensing eavesdropping SCNR constraint in the proposed scheme to ensure sensing security. Regarding Fig. 4, it can be found that when $\gamma_{se} = 2\text{ dBm}$, the value of γ_s at which the feasibility probability becomes 0 is approximately 29.2 dBm. When $\gamma_{se} = 5\text{ dBm}$, the value of γ_s at which the feasibility probability becomes 0 is approximately 32.2 dBm. That is to say, when the sensing security requirement becomes more stringent, the achievable highest sensing performance becomes lower. Combining the analysis of Fig. 3 and Fig. 4, we can see that the presence of sensing security constraint imposes a certain limitation on the sensing performance. When the system requires higher sensing performance, it faces a higher risk of sensing eavesdropping. There is a tradeoff between sensing security and sensing performance. To verify the superiority of the proposed scheme, it is compared with the

Fig. 4. The feasibility probability v.s. γ_s

random sensing signal covariance matrix scheme, denoted as “S Random”, where the optimization problem (P4) is solved regarding \mathbf{Q}_k only using the SCA without optimizing the sensing signal covariance matrix \mathbf{S} . \mathbf{S} is randomly generated and guaranteed to be within the maximum BS transmit power constraint.

To investigate the impact of BS transmit power on the communication security performance, the system secrecy rate under different transmit powers is simulated. The number of antennas $N_t = 8$, $N_t = 10$, $N_t = 12$. The BS SCNR threshold $\gamma_s = 32\text{ dBm}$. The sensing eavesdropper SCNR threshold $\gamma_{se} = 5\text{ dBm}$. With respect to Fig. 5, it can be found that the system secrecy rate increases with the incremental of maximum BS transmit power. Increasing the power resource can achieve higher communication security performance. Additionally, compared to the baseline scheme “S Random”, the proposed algorithm reaches better communication security performance. For example, when $N_t = 8$ and $P = 18\text{dBm}$, the system secrecy rate of the proposed scheme is increased by approximately 98.3% compared to “S Random”. It is because that the joint optimization of sensing signal covariance matrix and the communication signal covariance matrix leads to optimal system power allocation. The interference from the sensing signal to communications can be minimized, while the interference to the communication eavesdropper is maximized, thereby the proposed scheme optimizes the communication security. Regarding the “S Random” scheme, \mathbf{S} is randomly generated, and it cannot coordinate the resource allocation between communication and sensing. This results in excessive interference to CUs or insufficient interference to communication eavesdroppers. Therefore, the system secrecy rate achieved by the proposed scheme is significantly faster than the “S Random” scheme, which demonstrates the superiority of the proposed algorithm. Furthermore, we can see that increasing the number of BS transmit antennas leads to higher system secrecy rate, it is because that the increment of N_t provides the system with higher spatial degrees of freedom.

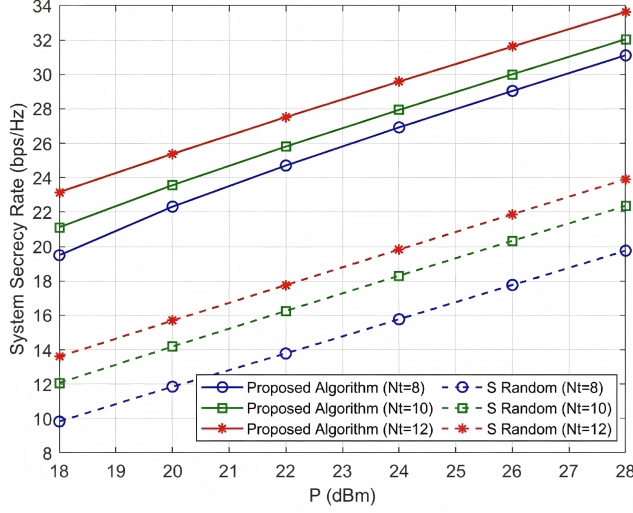


Fig. 5. System secrecy rate v.s. maximum BS transmit power

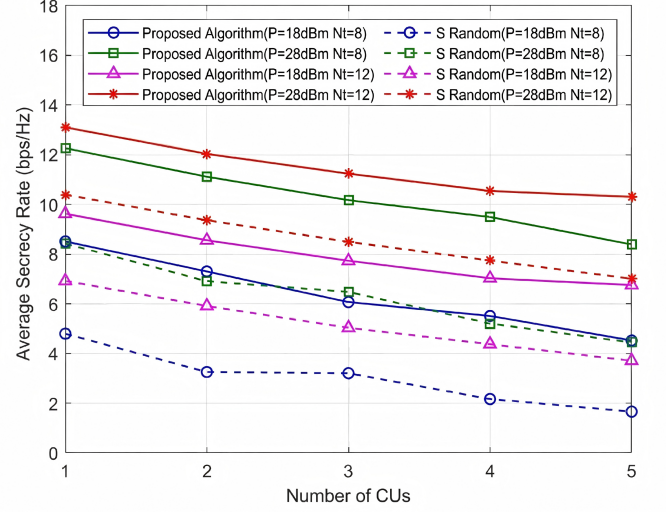
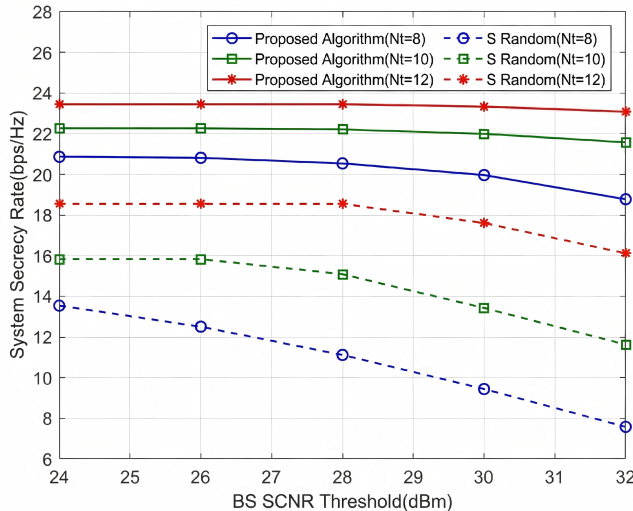
Fig. 7. Average secrecy rate v.s. K Fig. 6. System secrecy rate v.s. γ_s

Fig. 6 illustrates the system secrecy rate performance regarding the BS SCNR threshold, γ_s , given BS transmit power, where we can analyze the trade-off between sensing performance and communication security in the ISAC system. The BS antenna numbers $N_t = 8$, $N_t = 10$, the transmit power $P = 18$ dBm, and the sensing eavesdropper SCNR threshold $\gamma_{sc} = 5$ dBm. It can be observed that system secrecy rate decreases with the increase of γ_s . This is because when the system's power resources are fixed, an increase in the BS SCNR threshold leads to more power allocation for sensing, and relatively less to communication, resulting in the decline in communication security performance. Therefore, under limited power resources, the ISAC system needs to balance between sensing performance and communication performance. Furthermore, it is also found that when N_t is larger, the system secrecy rate decreases relatively slower. With the increment of γ_s from 24 dBm to 32 dBm, the system secrecy rate decreases

approximately 2.1 bps/Hz for $N_t = 8$, approximately 0.7 bps/Hz for $N_t = 10$, and approximately 0.4 bps/Hz for $N_t = 12$. The reason is that larger number of BS transmit antennas provides higher spatial degrees of freedom, which can mitigate the negative impact on communication security, i.e., the increased power resource occupation for improving sensing performance. Fig. 7 demonstrates the average secrecy rate with respect to the number of CUs, K , given BS transmit power and number of transmit antennas. The BS transmit power $P = 18$ dBm and $P = 28$ dBm, the BS antenna number $N_t = 8$ and $N_t = 12$, the BS SCNR threshold $\gamma_s = 32$ dBm, and the sensing eavesdropper SCNR threshold $\gamma_{sc} = 5$ dBm. It can be observed that the average secrecy rate of the proposed scheme decreases significantly when the number of users increases. This indicates that when the system power resource and antenna resource are fixed, an increase in the number of users requiring resource allocation leads to a reduction in the average communication security performance. Furthermore, comparing different lines, we can find that the average communication security performance can be improved by increasing the system's transmit power or the number of transmit antennas.

The normalized beam pattern gain of communication signal and the sensing signal can be respectively given by

$$\begin{aligned} P_c(\theta) &= \mathbb{E} \left[\left| \mathbf{a}^H(\theta) \mathbf{W} \mathbf{c} \right|^2 \right] = \mathbf{a}^H(\theta) \sum_{k=1}^K w_k w_k^H \mathbf{a}(\theta) \\ &= \mathbf{a}^H(\theta) \sum_{i=1}^K \mathbf{Q}_i \mathbf{a}(\theta) \end{aligned} \quad (50)$$

and

$$P_s(\theta) = \mathbb{E} \left[\left| \mathbf{a}^H(\theta) \mathbf{s} \right|^2 \right] = \mathbf{a}^H(\theta) \mathbf{S} \mathbf{a}(\theta). \quad (51)$$

Fig. 8 and Fig. 9 show the normalized beam pattern gain of the proposed beamforming algorithm regarding θ under the AoA of the sensing target $\theta_t = 0^\circ$ and $\theta_t = 10^\circ$, respectively. As can be observed from the figures, in the

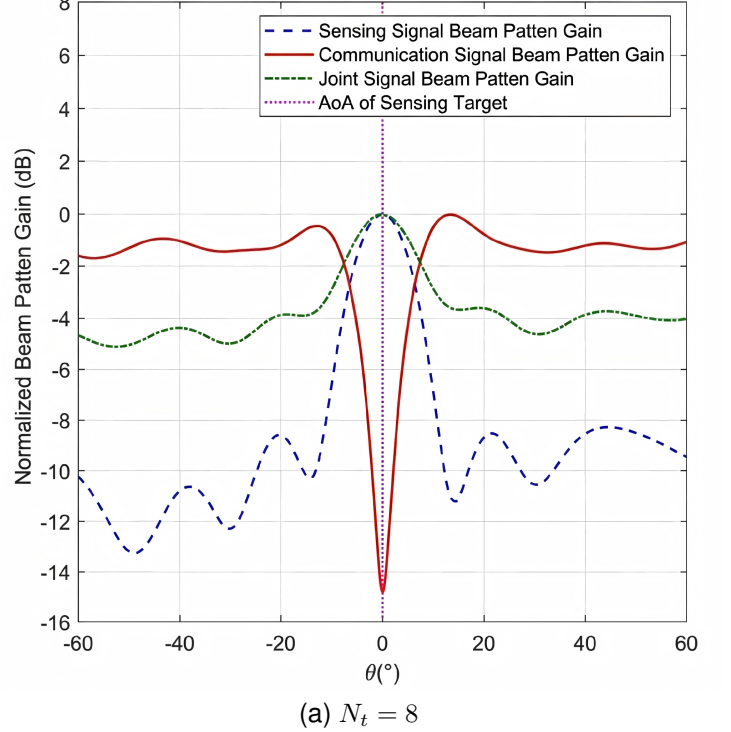
direction of the sensing target θ_t , the beam pattern gain of the sensing signal is the highest, while the beam pattern gain of the communication signal exhibits a sharp decrease. This indicates that, through the joint optimization of the sensing signal covariance matrix \mathbf{S} and the communication signal covariance matrices \mathbf{Q}_k , the BS is able to concentrate the transmitted sensing signal primarily in the direction of the sensing target. In this way, the proposed beamforming algorithm not only fulfills the sensing functionality but also acts as artificial noise to prevent eavesdropping by potential communication eavesdroppers. Furthermore, the energy of the communication signal is minimized in this direction, thereby demonstrating the effectiveness of the proposed beamforming scheme in ensuring communication security. Additionally, by comparing Fig. 8a with Fig. 8b or Fig. 9a with Fig. 9b, it can be seen that the main lobe width of the sensing signal beam for $N_t = 12$ is narrower than $N_t = 8$, and the sidelobe gain is also significantly lower. This shows that increasing the number of transmit antennas at the BS can achieve better orientation and higher angular resolution during sensing, more precise energy concentration in the direction of the sensing target and reduction of interference in other directions can be obtained.

V. CONCLUSION

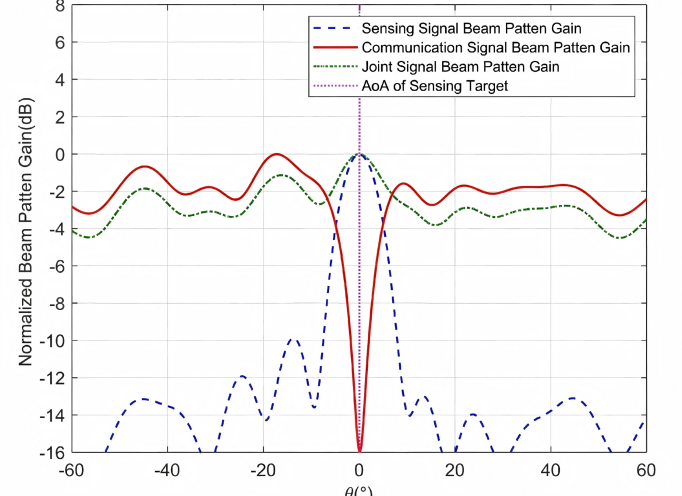
Both communication and sensing eavesdroppers are taken into consideration in ISAC systems. By optimizing the transmit communication signal and sensing signal beamforming covariance matrices, the system secrecy rate is maximized under SCNR constraints at the BS and at potential sensing eavesdropper as well as the transmit power constraint. The SCA is applied to handle the formulated non-convex optimization problem. The first-order Taylor expansion together with the SDR is utilized. In addition, we theoretically prove that the SDR produces no sub-optimality in the paper. The iterative secure beamforming algorithm against communication and sensing eavesdroppers is designed finally. Simulations are carried out to verify the effectiveness and superiority of the proposed scheme.

APPENDIX PROOF OF LEMMA 1

Since the optimization problem (P4) is the relaxation of the optimization problem (P3) by omitting Eq. (22), i.e., the rank one constraint of \mathbf{Q}_k , we prove the lemma by verifying that the optimal solution \mathbf{Q}_k^* of (P4) satisfies Eq. (22), i.e., $\text{rank}(\mathbf{Q}_k^*) = 1$. For convenience in the subsequent proof, we transform the maximization problem into a minimization form, which does not affect the optimal solution. (P4) is convex with respect to all optimization variables and satisfies the Slater condition. Therefore, strong duality holds for the relaxed problem, i.e., the gap between the optimal value of (P4) and



(a) $N_t = 8$



(b) $N_t = 12$

Fig. 8. The normalized beam pattern gain of the proposed beamforming algorithm when $\theta_t = 0^\circ$

the optimal value of its dual problem is zero. The Lagrangian

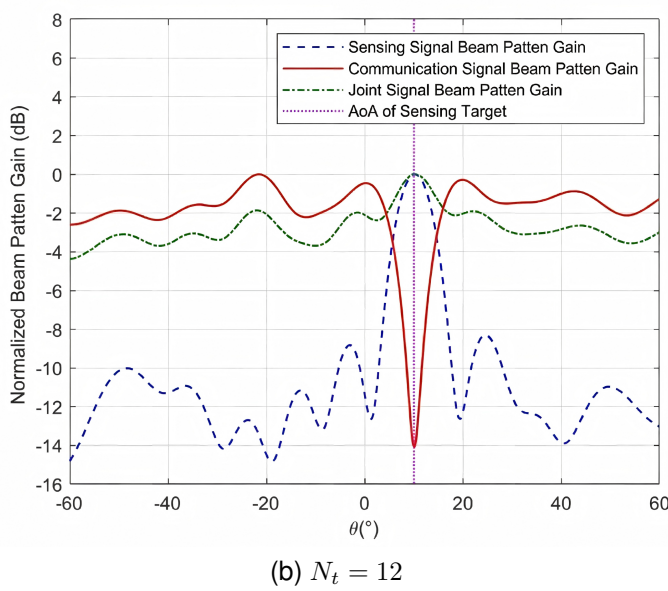
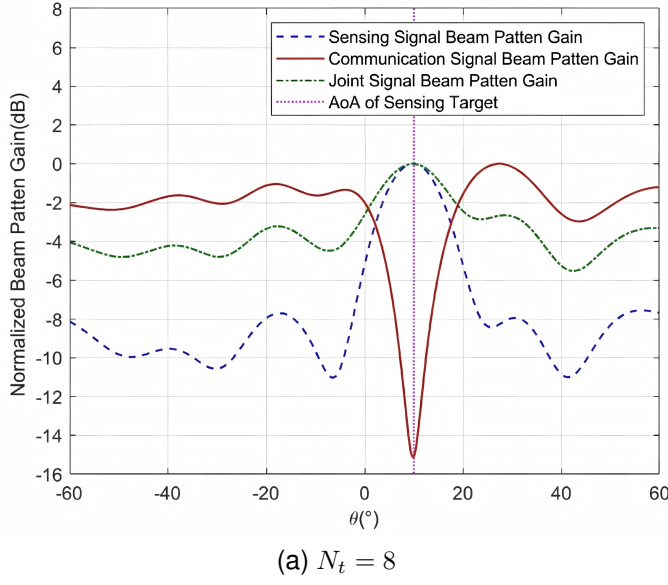


Fig. 9. The normalized beam pattern gain of the proposed beamforming algorithm when $\theta_t = 10^\circ$

function \mathcal{L} of optimization problem (P4) can be given by

$$\begin{aligned} \mathcal{L} = & r \text{Tr} \left(\sum_{k=1}^K \mathbf{Q}_k \right) + m_1 \sum_{k=1}^K t_k \left(\mathbf{h}_{\text{se},k} \mathbf{Q}_k \mathbf{h}_{\text{se},k}^H - \gamma_{\text{se}} \right) \quad (52) \\ & \times \sum_{i=1, i \neq k}^K \mathbf{h}_{\text{se},k} \mathbf{Q}_i \mathbf{h}_{\text{se},k}^H \right) + p \gamma_s m_3 \sum_{k=1}^K \text{Tr} \left(\mathbf{H}_{\text{ce}} \mathbf{Q}_k \mathbf{H}_{\text{ce}}^H \right) - \\ & m_1 \sum_{k=1}^K \xi_{1,k} \sum_{i=1}^K \mathbf{h}_k \mathbf{Q}_i \mathbf{h}_k^H - m_2 \sum_{k=1}^K \xi_{2,k} \sum_{i=1, i \neq k}^K \mathbf{h}_{\text{ce}}^H \mathbf{Q}_i \\ & \times \mathbf{h}_{\text{ce}} + m_1 \sum_{k=1}^K \xi_{3,k} \sum_{i=1, i \neq k}^K \mathbf{h}_k \mathbf{Q}_i \mathbf{h}_k^H + m_2 \sum_{k=1}^K \xi_{4,k} \\ & \times \sum_{i=1, i \neq k}^K \mathbf{h}_{\text{ce}}^H \mathbf{Q}_i \mathbf{h}_{\text{ce}} - \sum_{k=1}^K \text{Tr} \left(\mathbf{Q}_k \mathbf{Y}_k \right) + \Upsilon, \quad (53) \end{aligned}$$

where Υ denotes the sum of all terms unrelated to \mathbf{Q}_k , r , t_k , p , $\xi_{1,k}$, $\xi_{2,k}$, $\xi_{3,k}$, $\xi_{4,k}$ are the Lagrangian multipliers introduced by constraints (29), (27), (28), (36), (39), (42), and (43), respectively, and they are non-negative. $\mathbf{Y}_k \in \mathbb{C}^{N_t \times N_t}$ denotes the Lagrangian multiplier matrix introduced by constraint (23), which is a positive semidefinite matrix. The Lagrangian dual problem of optimization problem (P4) can be given by

$$\max_{r, t_k, p, \xi_{1,k}, \xi_{2,k}, \xi_{3,k}, \xi_{4,k} \geq 0, \mathbf{Y}_k \succeq 0} \quad \min_{\{\mathbf{Q}_k\}_{k=1}^K, \mathbf{S}, u, \{\tau_k, \varepsilon_k, v_k\}_{k=1}^K} \mathcal{L}. \quad (54)$$

Applying the Karush-Kuhn-Tucker (KKT) conditions regarding \mathbf{Q}_k , we have

$$\begin{cases} r^*, t_k^*, p^*, \xi_{1,k}^*, \xi_{2,k}^*, \xi_{3,k}^*, \xi_{4,k}^* \geq 0, \text{ and } \mathbf{Y}_k^* \succeq \mathbf{0}, & (55) \\ \mathbf{Y}_k^* \mathbf{Q}_k^* = \mathbf{0}, & (56) \\ \nabla_{\mathbf{Q}_k^*} \mathcal{L} = \mathbf{0}, & (57) \end{cases}$$

where r^* , t_k^* , p^* , $\xi_{1,k}^*$, $\xi_{2,k}^*$, $\xi_{3,k}^*$, $\xi_{4,k}^*$, and \mathbf{Y}_k^* represent the optimal Lagrangian multipliers. The gradient of the Lagrangian function \mathcal{L} with respect to \mathbf{Q}_k^* , $\nabla_{\mathbf{Q}_k^*} \mathcal{L}$, is derived by

$$\begin{aligned} \nabla_{\mathbf{Q}_k^*} \mathcal{L} = & r^* \mathbf{I}_{N_t} + m_1 \sum_{k=1}^K \left(t_k^* \mathbf{h}_{\text{se},k}^H \mathbf{h}_{\text{se},k} - \gamma_{\text{se}} \right. \\ & \times \left. \sum_{i=1, i \neq k}^K t_i^* \mathbf{h}_{\text{se},i}^H \mathbf{h}_{\text{se},i} \right) + p^* \gamma_s m_3 \mathbf{H}_{\text{ce}}^H \mathbf{H}_{\text{ce}} \\ & - m_1 \sum_{k=1}^K \xi_{1,k}^* \mathbf{h}_k^H \mathbf{h}_k - m_2 \sum_{k=1}^K \sum_{i=1, i \neq k}^K \xi_{2,i}^* \mathbf{h}_{\text{ce}} \mathbf{h}_{\text{ce}}^H \\ & + m_1 \sum_{k=1}^K \sum_{i=1, i \neq k}^K \xi_{3,i}^* \mathbf{h}_i^H \mathbf{h}_i + m_2 \sum_{k=1}^K \sum_{i=1, i \neq k}^K \xi_{4,k}^* \\ & \times \mathbf{h}_{\text{ce}} \mathbf{h}_{\text{ce}}^H - \mathbf{Y}_k^*. \quad (58) \end{aligned}$$

Since the power constraint (29) holds with equality for \mathbf{Q}_k^* , the corresponding Lagrangian multiplier satisfies $r^* > 0$. Consequently, we can obtain

$$\mathbf{Y}_k^* = r^* \mathbf{I}_{N_t} - \Delta_k^*, \quad (59)$$

where

$$\begin{aligned} \Delta_k^* = & -m_1 \sum_{k=1}^K \left(t_k^* \mathbf{h}_{\text{se},k}^H \mathbf{h}_{\text{se},k} - \gamma_s \sum_{i=1, i \neq k}^K t_i^* \mathbf{h}_{\text{se},i}^H \mathbf{h}_{\text{se},i} \right) \\ & - p^* \gamma_s m_3 \mathbf{H}_{\text{ce}}^H \mathbf{H}_{\text{ce}} + m_1 \sum_{k=1}^K \xi_{1,k}^* \mathbf{h}_k^H \mathbf{h}_k + m_2 \\ & \times \sum_{k=1}^K \sum_{i=1, i \neq k}^K \xi_{2,i}^* \mathbf{h}_{\text{ce}} \mathbf{h}_{\text{ce}}^H - m_1 \sum_{k=1}^K \sum_{i=1, i \neq k}^K \xi_{3,i}^* \mathbf{h}_i^H \mathbf{h}_i \\ & - m_2 \sum_{k=1}^K \xi_{4,k}^* \mathbf{h}_{\text{ce}} \mathbf{h}_{\text{ce}}^H. \end{aligned}$$

Let $v_{\Delta_k^*}^{\max} \in \mathbb{R}$ denote the maximum eigenvalue of the matrix Δ_k^* . Due to the randomness of the channel, the probability that multiple eigenvalues are equal to $v_{\Delta_k^*}^{\max}$ is zero [25]. Therefore, $v_{\Delta_k^*}^{\max}$ is unique. We analyze the magnitude of the eigenvalues of the two terms on the right-hand side of Eq. (59). If $r^* < v_{\Delta_k^*}^{\max}$, then the matrix \mathbf{Y}_k^* would have

negative eigenvalues, contradicting the condition $\mathbf{Y}_k^* \succeq \mathbf{0}$. Hence, $r^* \geq v_{\Delta_k^*}^{\max}$. Specifically, when $r^* = v_{\Delta_k^*}^{\max}$, the matrix \mathbf{Y}_k^* has one zero eigenvalue and $(N_t - 1)$ eigenvalues greater than zero. When $r^* > v_{\Delta_k^*}^{\max}$, all N_t eigenvalues of \mathbf{Y}_k^* are positive. That is to say, the matrix \mathbf{Y}_k^* has at least $(N_t - 1)$ eigenvalues greater than zero, which implies that $\text{rank}(\mathbf{Y}_k^*) \geq N_t - 1, \forall k$. Furthermore, according to the complementary slackness condition (56) and the rank-nullity theorem, $\text{rank}(\mathbf{Y}_k^*) + \text{nullity}(\mathbf{Y}_k^*) = N_t$, where $\text{nullity}(\mathbf{Y}_k^*)$ denotes the dimension of the null space of \mathbf{Y}_k^* . Accordingly, $\text{nullity}(\mathbf{Y}_k^*) \leq 1$, and thereby $\text{rank}(\mathbf{Q}_k^*) \leq 1$. According to the physical meaning of the communication system, \mathbf{Q}_k^* is not the zero matrix, so it satisfies $\text{rank}(\mathbf{Q}_k^*) = 1$. Together with the strong duality of the relaxed problem, it is proven that the solution \mathbf{Q}_k of optimization problem (P4) satisfies $\text{rank}(\mathbf{Q}_k) = 1, \forall k$. This complete the proof.

Remark: Based on the above analysis, we can construct a bounded optimal solution. Specifically, we first define a unit-norm vector $\mathbf{e}_k^{\max} \in \mathbb{C}^{N_t \times 1}$ that lies in the null space of \mathbf{Y}_k^* , satisfying $\mathbf{Y}_k^* \mathbf{e}_k^{\max} = \mathbf{0}$. This unit-norm vector is associated with the maximum eigenvalue v_k^{\max} of \mathbf{Y}_k^* . Therefore, the optimal solution \mathbf{Q}_k^* can be expressed as

$$\mathbf{Q}_k^* = \varpi \mathbf{e}_k^{\max} (\mathbf{e}_k^{\max})^H,$$

where the parameter ϖ can be adjusted to satisfy the transmit power constraint (29).

REFERENCES

- [1] F. Liu et al., "Integrated sensing and communications: Toward dual-functional wireless networks for 6G and beyond," *IEEE Journal on Selected Areas in Communications*, vol. 40, no. 6, pp. 1728-1767, June 2022.
- [2] N. González-Prelcic et al., "The Integrated sensing and communication revolution for 6G: Vision, techniques, and applications," *Proceedings of the IEEE*, vol. 112, no. 7, pp. 676-723, July 2024.
- [3] D. Zhang et al., "Integrated sensing and communications over the years: An evolution perspective," in *IEEE Communications Surveys & Tutorials*, doi: 10.1109/COMST.2026.3655674, 2026, to appear.
- [4] X. Gan et al., "Coverage and rate analysis for integrated sensing and communication networks," *IEEE Journal on Selected Areas in Communications*, vol. 42, no. 9, pp. 2213-2227, Sept. 2024.
- [5] M. Mei, M. Yao, Q. Yang, J. Wang, Z. Jing and T. Q. S. Quek, "Network-layer delay provisioning for integrated sensing and communication UAV networks under transient antenna misalignment," *IEEE Transactions on Wireless Communications*, vol. 23, no. 10, pp. 12964-12979, Oct. 2024.
- [6] W. Hong et al., "Integrated sensing and communication (ISAC) channel model towards 3GPP 6G standardization: Modelling, validation, and application," *IEEE Journal on Selected Areas in Communications*, doi: 10.1109/JSAC.2026.3656257, to appear.
- [7] M. E. Benattia, S. E. Zegrar and H. Arslan, "Analog assisted OFDM receiver with ultra-low-rate ADCs for ISAC systems," *IEEE Wireless Communications Letters*, doi: 10.1109/LWC.2026.3662445, 2026, to appear.
- [8] B. Mukhiddinov, D. He and W. Yu, "Optimizing sensing and communication trade-offs in MIMO: A hybrid approach for 6G ISAC systems," *IEEE Transactions on Vehicular Technology*, doi: 10.1109/TVT.2025.3628170, to appear.
- [9] O. Günlü, M. R. Bloch, R. F. Schaefer and A. Yener, "Secure integrated sensing and communication," *IEEE Journal on Selected Areas in Information Theory*, vol. 4, pp. 40-53, 2023.
- [10] A. Bazzi and M. Chafii, "Secure full duplex integrated sensing and communications," *IEEE Transactions on Information Forensics and Security*, vol. 19, pp. 2082-2097, 2024.
- [11] X. Zhang, W. Jiao, W. Liu and C. Qi, "Energy efficiency optimization in secure full-duplex ISAC systems," *IEEE Communications Letters*, vol. 29, no. 1, pp. 220-224, Jan. 2025.
- [12] Y. Cao, L. Duan and R. Zhang, "Sensing for secure communication in ISAC: Protocol design and beamforming optimization," *IEEE Transactions on Wireless Communications*, vol. 24, no. 2, pp. 1207-1220, Feb. 2025.
- [13] A. A. Al-Habob, O. A. Dobre and Y. Jing, "Predictive beamforming approach for secure integrated sensing and communication with multiple aerial eavesdroppers," *IEEE Transactions on Communications*, vol. 73, no. 9, pp. 7887-7898, Sept. 2025.
- [14] Z. Chen, S. Zhu and X. Li, "Near-field assisted secure ISAC system: Synergistic enhancement between sensing and secure transmission," *IEEE Communications Letters*, vol. 29, no. 10, pp. 2268-2272, Oct. 2025.
- [15] Z. Chen, F. Wang, G. Han, X. Wang and V. K. N. Lau, "Robust beamforming design for secure near-field ISAC systems," *IEEE Wireless Communications Letters*, vol. 14, no. 10, pp. 3089-3093, Oct. 2025.
- [16] F. Liu, J. Mu, W. Xu, J. Miao, W. Bazzi and S. Mumtaz, "Toward secure and energy-efficient ISAC in low-altitude IoT: A game-theoretic DRL framework with adaptive sensing," *IEEE Internet of Things Journal*, vol. 12, no. 24, pp. 53202-53214, Dec. 2025.
- [17] B. Hua, H. Peng, Z. Li, N. Cheng, K. Zhang and Z. Su, "Joint dynamic tracking and robust secure beamforming for full-duplex ISAC systems," *IEEE Transactions on Wireless Communications*, vol. 25, pp. 8614-8628, 2026, doi: 10.1109/TWC.2025.3640414, to appear.
- [18] H. Lei, H. Jin, K. -H. Park, M. A. Aboulhassan, X. Miao and G. Pan, "On secure UAV-aided ISAC system via sensing," *IEEE Internet of Things Journal*, doi: 10.1109/IOT.2026.3660355, 2026, to appear.
- [19] F. Jia, A. Li, X. Liao, Y. Li and C. Masouros, "Secure precoding via interference exploitation in integrated sensing and communication system," *IEEE Wireless Communications Letters*, vol. 15, pp. 425-429, 2026, doi: 10.1109/LWC.2025.3625406, to appear.
- [20] C. Yin, P. Gong, M. Luo, Y. Wu, Z. Zhang and L. Zeng, "Secure waveform design for mimo integrated sensing and communication under the stochastic TIR model," *IEEE Internet of Things Journal*, doi: 10.1109/IOT.2025.3650625, 2026, to appear.
- [21] Y. Zhang, B. Wang, G. Ding, W. Yuan, A. Liu and B. Ren, "ISAC-assisted covert transmission: Joint secure sensing and communication," *IEEE Journal on Selected Areas in Communications*, doi: 10.1109/JSAC.2025.3637793, 2026, to appear.
- [22] Z. Ren, J. Xu, L. Qiu and D. Wing Kwan Ng, "Secure cell-free integrated sensing and communication in the presence of information and sensing eavesdroppers," *IEEE Journal on Selected Areas in Communications*, vol. 42, no. 11, pp. 3217-3231, Nov. 2024.
- [23] J. Zou, C. Masouros, F. Liu and S. Sun, "Securing the sensing functionality in ISAC networks: An artificial noise design," *IEEE Transactions on Vehicular Technology*, vol. 73, no. 11, pp. 17800-17805, Nov. 2024.
- [24] K. Han, K. Meng and C. Masouros, "Sensing-secure ISAC: Ambiguity function engineering for impairing unauthorized sensing," *IEEE Transactions on Wireless Communications*, vol. 25, pp. 5386-5400, 2026, doi: 10.1109/TWC.2025.3618121, to appear.
- [25] D. Xu, X. Yu, Y. Sun, D. W. K. Ng and R. Schober, "Resource allocation for IRS-assisted full-duplex cognitive radio systems," *IEEE Transactions on Communications*, vol. 68, no. 12, pp. 7376-7394, Dec. 2020.